13th ewtec 2019 Proceedings of the 13th European Wave and Tidal Energy Conference 1-6 Sept 2019, Naples, Italy

Energy harvesting from waves using tandem floaters connected by piezoelectric beams

Daniele Dessi, Giorgia Leonardi, and Fabio Passacantilli

***Abstract*—In this paper, a small-scale floating system capable to extract energy from the waves is presented. The prototype floating structure consists of two box-shaped bodies joined by flexible beams and keeps its position with respect to the seabed via mooring lines. Due to the wave excitation, the platforms experience relative pitch rotations, and the mechanical energy related to this relative motion is then converted in electrical energy using a power take-off system based on piezoelectric beams.**

A simple experiment is arranged to demonstrate the feasibility of the concept and to obtain data to validate the numerical model. Two floaters are built in plastic materials, linked to each other with commercial PZT piezoelectric harvesters. The regular-wave tests are carried out in a small basin with a plunge wavemaker properly designed to produce a small wave amplitude suitable for the physical model dimension. The experimental data relative to the floater motion is used as input to calculate the tip displacement of the flexible element reproducing the mechanical behaviour of the real PZT device. The tip displacement time-history then serves as input to calculate the voltage output of the connecting piezoelectric device via a numerical model developed with a multiphysics software.

***Index Terms*—Wave energy converters, piezoelectric power-take-off, small-scale tests.**

I. Introduction

In the last years, to exploit the huge energy potential carried by surface waves, a multitude of Wave Energy Converters have been conceived, leading to different engineering solutions in terms of mechanical configurations and power take-off systems. The wave-energy converter proposed in this article is based on a segmented layout made of floaters linked to each other in a row, subjected to wave excitation, and kept in position with respect to the seabed by using mooring lines. This specific structure can be found in previous works, such as DUCK [1], LEANCON [2], Pelamis [3], SeaBeavl [4], and DEXAwave [2]. In particular, the last one (the most similar to the device presented in this paper) is made of two platforms hinged, whose relative pitch activates a low pressure power transmission. However, all the WEC mentioned above suffer from complex electro-mechanical PTO systems, difficult maintenance in offshore conditions, and high production costs. All these facts lead to investigations on more easy, reliable, and cheap PTOs, based, among the others, on piezoelectric direct energy conversion from fluid. In their review paper [5], Jbaily and Yeung gave a comprehensive overview about the rising interest toward piezo-based PTOs, as demonstrated by the large number of different configurations reported. For instance, Carroll [6] uses PVDF (Polyvinylidene Fluoride, a poled electroactive polymer) to transform vortices induced by bluff bodies or fluid kinetic energy into electricity. Koca's device [7] simply exploits wave impacts on piezoceramic surfaces to produce energy. Similarly, there are WECs with flexible surfaces stimulated by pressure oscillations [8] or beams clamped to the sea bed [9] - [10] miming seaweeds motion in shallow water. Another device with a piezo PTO that has been studied by several authors [11]- [12]- [13]- [14] consists in a buoy with an internal pendulum mechanism that impacts on piezoceramic elements. The pendulum oscillation converts the low wave frequency into higher frequencies, more suitable to induce resonance in piezoelectric components, with consequential increase in energy production. Similar to this configuration is the buoy designed by Viet [15], which exploits the pitch motion to move an internal magnetic bar, that induces vibrations in the cantilevered piezoelectric elements. Moreover, in [16] semi-submerged plates have been tested under wave excitation, analysing the mechanical coupling with piezoelectric films. This device, suitable in general to host any kind of conversion system (see [17]), combines a piezoelectric PTO with the concept of a segmented floating structure.

In this paper the authors aim at investigating the potential of an elementary modular WEC device, constituted by a segmented floating structure of two box-shaped bodies as in the considered case, but replicable several times to form wide arrays (Fig 1). The moored floaters are joined by flexible connections, which allow relative heave and pitch motions but exerting at the same time restoring forces and moments. Piezoelectric elements are embedded at these connections and are actuated by the relative motion of the adjacent bodies under wave excitation, producing electrical energy.

As a second step after setting a numerical model of the system [18], the feasibility of the proposed concept is investigated experimentally by testing at small scale two floating bodies linked with a elastic elements having globally a bending flexibility close to a commercially available piezoelectric bender with the same dimensions. The tests, carried out in a small basin with regular waves of about 1 cm amplitude, exploit an

ID 1809-WDD.

D. Dessi is with the Marine Technology Research Institute of National Research Council (CNR-INM) 00128 Via di Vallerano 139 Rome, Italy (e-mail: daniele.dessi@cnr.it).

G. Leonardi is a PhD student at the University of Rome "La Sapienza" under CNR-INM scholarship 00128 Via di Vallerano 139 Rome, Italy (e-mail: giorgia.leonardi@uniroma1.it).

F. Passacantilli was with the Institute of Science and Technology of Ceramics, now he is has a scholarship with CNR-INM, 00128 Via di Vallerano 139 Rome, Italy (e-mail: fabio.passacantilli@istec.cnr.it).

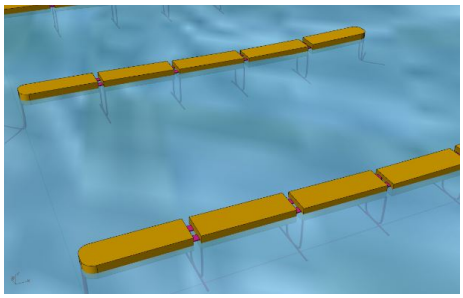

Fig. 1. WEC concept based on floater connected with piezoelectric beams.

innovative way of building the physical models using LEGO bricks and on-board low-weight IMUs to record the motions. This way of building the physical models will allow for changing easily the floater configuration in the future. The response amplitude operators of the absolute and relative motion of the floaters under regular wave excitation are obtained for typical wave lengths. The data collected are then used as input of a multiphysics model of the selected piezoelectric benders, obtaining the voltage output.

II. CONCEPT DEVICE

As stated in the introduction, the device analysed in this paper is the basic module of a more complex WEC based on several box-shaped slender floaters. In its simplest arrangement, the floaters are linked on the short side with hinge-like connections made of flexible bars as shown in Fig. 1; thus, the device is designed to better perform with the main axis aligned with the wave direction, since the PTO exploits the relative pitch motion between the two bodies. For this reason, at full-scale mooring lines are needed to keep the whole system in a certain position, and a proper mooring layout or mechanism supporting the correct alignment with respect to the wave and wind directions is required; it will be implemented in further studies. The shape and dimension of the floaters may vary depending on several factors, like technological issues, characteristic wave periods, PTO optimization, etc.. Moreover, the choice of building materials, carrying out the mechanical and chemical resistance to the sea environment, is another important step to make the device as reliable as possible, and then to reduce the risk of structural failures as well as the need for maintenance. As mentioned before, the connections between the floaters are provided by flexible beams, represented in Fig. 1 as purple elements between the floaters, over which the piezoelectric devices are fixed (glued, embedded, etc.). Insulation and protection of all electrical components (cabling, contacts, piezoelectrics) from the external environment is one of the most critical issues of this system. On the other hand, the PTO has the advantage to be simple both electrically and mechanically, if compared, for instance, to pneumatic circuits typical of traditional WEC devices. As a first step toward future technological improvements and layout optimization, in this experimental campaign the two floating bodies have been constructed with a a ratio between the box-shape dimensions based on previous studies carried out on a similar segmented system [19].

TABLE I
MAIN DIMENSIONS OF THE FLOATING SYSTEM

Symbol	Quantity	Unit
L_{wec}	Overall length	0.829 m
L_{float}	Floater length	0.384 m
L_g	Gap between the floaters	0.061 m
b	Width	0.097 m
δ	Immersion	m
M_{tot}	Total mass	0.2 Kg
m_s	On-board sensor mass	0.1 Kg

III. TESTING SET-UP

The tested physical system is constituted by two box-shaped, elastically linked floating bodies of the same size whose principal dimensions are shown in Table I. The shape as well as the ratio between the length and the width of each floating body have been chosen to allow for a simple evaluation of the hydrodynamic forces via strip theory in the numerical model used for designing the set-up. As it emerges from Table I, the experiments are performed at small scale, without any scaling of a reference full-scale system. Testing small devices is the reason for building these devices with LEGO bricks (Fig. 2). In this way, in future testing we have chances to modify easily the floating system configuration in order to maximize the energy that can be extracted by the waves. The plastic construction of the floaters with LEGO bricks has needed to be properly sealed with silicon especially where small interstices between adjacent bricks were present. The elastic connection simulating the presence of the piezoelectric bender is done using LEGO elements as well, properly chosen between many alternatives to be similar to commercial benders.

The use of small floaters has important consequences on the set-up; for instance, insertion effects due to on-board sensors may become important and, at the same time, small-amplitude waves need to be realized. For this reason, the body motion is acquired with two Inertial Motion Units (IMUs): the first one is a device for accurate motion measurement, the second is a low-cost solution that has the advantage of having a disregardful weight (about 6 g). Each IMU, containing three accelerometers and three angular-speed transducers, give signals that are transformed into the time-history of generalized displacements by using proper software packages based on MATLAB routines. The sampling rate of the acquisition system is $100\ Hz$.

The small-scale basin (long $11.7\ m$, wide $1.44\ m$ and deep $1.57\ m$) is equipped with a plunge wavemaker properly sized to fit into the basin width (see Fig. 3) and to generate small waves. The wavemaker is not yet equipped with an electrical drive, limiting ourselves to the generation of regular waves alone with a manual crank. Nonetheless, thanks to some mechanical arrangements it allows producing a combination of wave

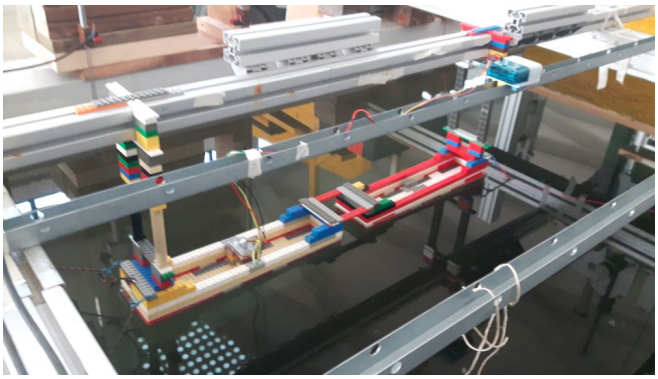

Fig. 2. Experimental setup.

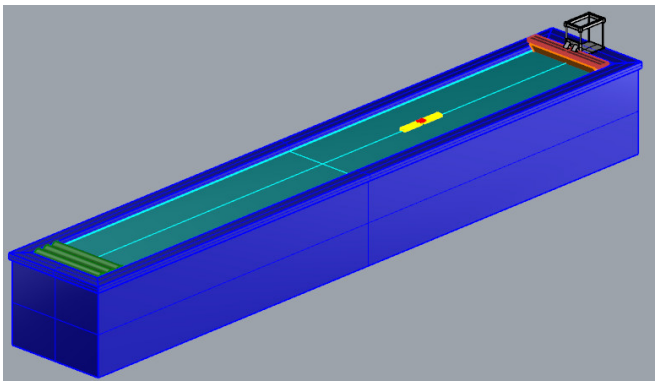

Fig. 3. Sketch of the wave basin arrangement.

amplitudes and frequencies acceptable for this first campaign also in terms of wave profile. The vertical motion of the plunging wedge was recorded with an accelerometer to track the precision of the wavemaker motion and have a real-time feedback on the wave generation features. The generated wave system was measured in two positions with capacitive wave probes placed at the mid-point of the floaters. The horizontal layout of the mooring lines allows for keeping the system aligned with the basin centerline. Special care was devoted to minimize the perturbation due to the IMU cables, which would require a characterization in terms of mass, stiffness and damping to be properly modelled in a numerical simulation. For this reason, a flexible suspension system was deployed to keep the cables in the right position and to provide negligible reaction forces and moments under floater motion.

IV. MODELLING

A 3D finite-element model of the piezoelectric PTO has been developed in COMSOL Multiphysics, simulating both the mechanical and the piezoelectric response. Piezoelectricity is the ability of a material to get polarized, producing a potential difference between two faces, when subjected to an external mechanical stress (direct effect) or, alternatively, to exhibit internal mechanical strain resulting from an applied electric field (converse effect). Both effects are useful for many applications, and in particular the direct effect is exploited for energy harvesting. The piezoelectricity state equations show the relation between mechanical and electrical behaviour in the material:

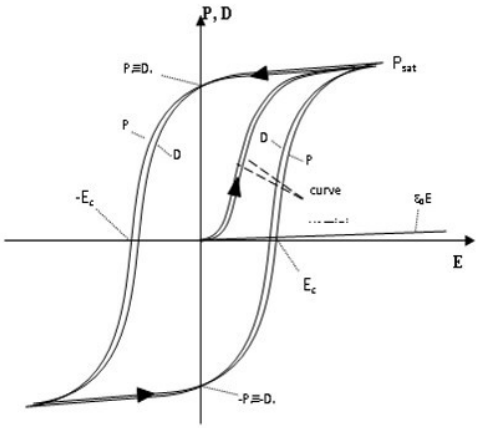

Fig. 4. Hysteresis cycle of a ferroelectric material.

$$\begin{aligned} S_{ij} &= s_{ijkl}\sigma_{kl} + d_{kij}E_k \\ D_i &= d_{ijk}\sigma_{jk} + \varepsilon_{ij}E_j \end{aligned} \tag{1}$$

where S is the strain, σ the stress, s the flexibility, d the piezoelectric coefficient and D is the electric displacement, E the electric field, ε the permittivity.

In more detail, the piezoelectric effect can occur under a uniform stress field due to the dissymmetric crystalline structure of this specific type of ceramics, which causes a non-zero total electric dipole moment in the material. In some cases piezoelectricity occurs naturally, like in quartz, but the most performing piezoelectric compounds, like PZT, are created from ferroelectric materials. These materials, similarly to what happens for ferromagnetics, show a total electric dipole equal to zero at the initial state, but their internal structure is organized in the so-called Weiss domains (zones with non-zero total dipole). When ferroelectric materials are subjected to an external electric field, their internal dipoles orientates in the field direction, generating a polarization up to the saturation of the material (i.e., when all the microscopical electric dipoles are oriented in the same way). This process is possible thanks to Weiss domains, that facilitate the change of orientation with respect to what would happen with a non-ferroelectric material. Since the polarization process occurs according to an hysteresis cycle (Fig. 4), when the external electric field goes to zero, a residual total electric dipole is still left into the material, that consequently shows piezoelectric properties.

The flexible beam junction and the piezoelectric elements are modelled in COMSOL, as shown in Fig. 5. The finite-element model has been used to predict voltage production and to verify that sea state conditions analysed could not damage the connections. The PTO has been simulated as a 3D bender plate, with one side clamped and the other free. To this edge, a displacement has been applied to simulate the relative motion between the floaters. Indeed, starting from experimental data, a relative displacement and pitch motion of one platform to another has been calculated at the interface of the body. In Table II are reported the

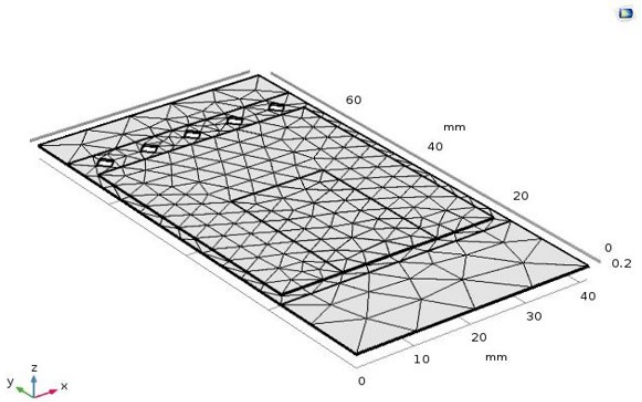

Fig. 5. 3D finite-element model of the PTO element in COMSOL Multiphysics.

input characteristic of the piezoelectric material acting as flexible beam junction between the floaters. The

TABLE II
PTO ELEMENT CHARACTERISTICS.

Mass [g]	m	6.0
Piezoelectric dimensions [mm]	LxHxT	$62x41.5x0.76$
Piezoelectric material		PZT 5H
Curie temperature [°C]	T_c	225
Bending stiffness [N/m]	D	250
Piezoelectric charge coefficient [C/N]	d_{31}	$-320 \cdot 10^{-12}$
Piezoelectric voltage coefficient [Vm/N]	g_{31}	$-9.5 \cdot 10^{-3}$

support layer thickness has been chosen to contain the neutral axis of the overall structure (Fig. 6), since this allows the piezoelectric material to be more uniformly stretched or shorten in the thickness direction. Indeed, if the neutral axis be placed inside the piezoelectric sheet, the material would have a partial or even total charge cancellation, and so a decreased power output.

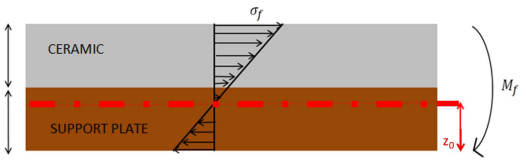

Fig. 6. Sketch of the optimal mechanical configuration.

V. RESULTS

Due to the imperfect characterization of the wave-maker transfer function, the wave elevation amplitude can be set only approximately during the test. Nonetheless, a complete series of regular wave tests with wave elevation around 0.014 m was achieved by discarding those tests where the standard deviation of the wave amplitude exceeded a given threshold. A similar approach was set for the wavelength even if, in that case, a greater precision can be obtained. The duration of each test is limited by the time instant at which the reflected waves come back from the beach to the physical model. To have a sufficient statistics, each test condition is repeated at least three times depending on the wave length.

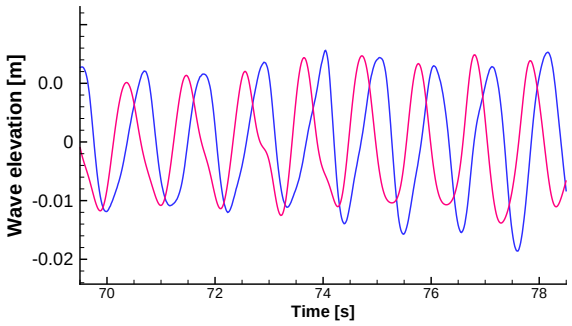

Fig. 7. Time history of regular wave amplitude ($a_w = 0.013$ and $\lambda_w/L_{wec} = 2.14$).

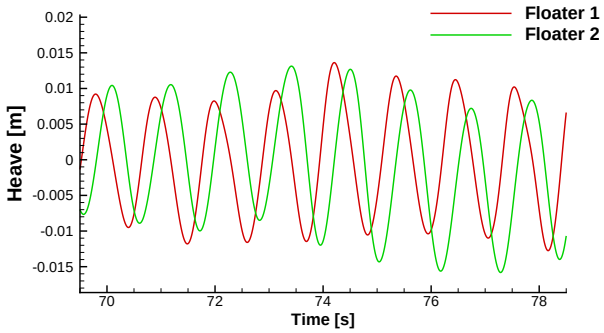

Fig. 8. Time history of heave response in regular waves ($a_w = 0.013$ and $\lambda_w/L_{wec} = 2.14$).

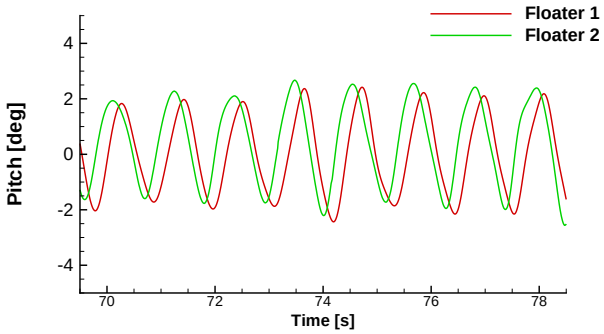

Fig. 9. Time history of pitch response in regular waves ($a_w = 0.013$ and $\lambda_w/L_{wec} = 2.14$).

The time history of wave, heave and pitch of the two floaters are shown in Figs. 7, 8 and 9 for the conditions $a_w = 0.013$ and $\lambda_w/L_{float} = 2.14$. There is a weak amplitude modulation of the wave elevation because of imperfect timing of the wedge motion which causes an energy leakage over the neighborhood of the nominal wave frequency. The second probe is partially affected by the diffraction of the incoming wave by the two floaters. However, the resulting effect on the two floaters response is rather small.

As an example of the dispersion around the nominal values of the wave parameters, the heave and pitch responses at model scale of the forward barge are plotted with respect to the measured wave length

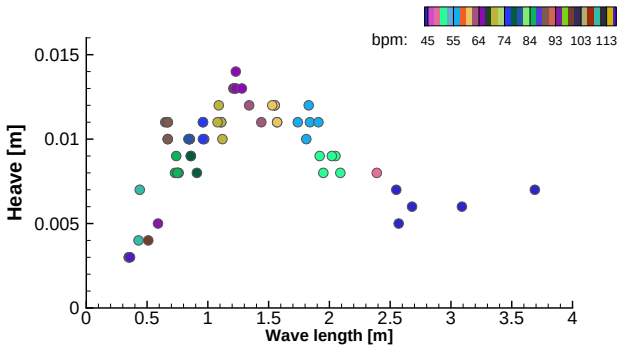

Fig. 10. Scatter plot of heave response of the forward floater in regular waves measured during tests.

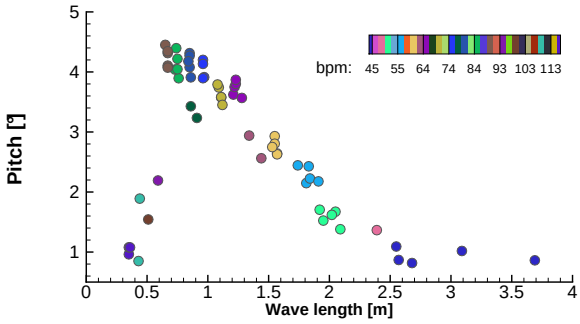

Fig. 11. Scatter plot of pitch response of the forward floater in regular waves measured during tests.

in Figs. 10 and 11, respectively. The same colours of adjacent points indicates that they are relative to tests characterized by the same oscillation frequency of the wavemaker wedge, expressed as the number of oscillation per minute.

The response amplitude operators (RAOs) in regular waves are then calculated according to the following definitions:

$$RAO_{heave} = \frac{z}{a_w}, \qquad RAO_{pitch} = \frac{\theta}{k_w\, a_w}, \tag{2}$$

with the wave number $k_w = 2\,\pi/\lambda_w$, being λ_w and a_w the wave length and elevation, respectively. The relative pitch rotation $\Delta\theta = \theta_1 - \theta_2$ between the two floaters is also defined, and the correspondent RAO is evaluated as:

$$RAO_{\Delta\theta} = \frac{\Delta\theta}{k_w\, a_w}, \tag{3}$$

It is worth to underline that the heave and pitch amplitude used for the calculation of RAO, as well as the wavelength, is obtained by averaging the values relative to the same nominal condition. The pitch RAO of the two floaters is similar for most wave lengths. On the other hand, the heave RAO appears to be slightly different, with that of the forward floaters larger at small wavelengths and slightly small as the wavelengths increase. A RAO secondary peak is clearly evident for $\lambda_w/L_{wec} = 0.84$ which corresponds to $\lambda_w/L_{float} = 1.6$, where L_{float} is the floater length; the same occurrence of the secondary peak was found previously in [18] for a geometrically similar configuration

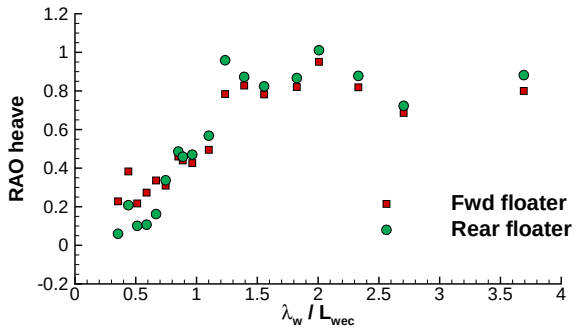

Fig. 12. Heave RAO in regular waves.

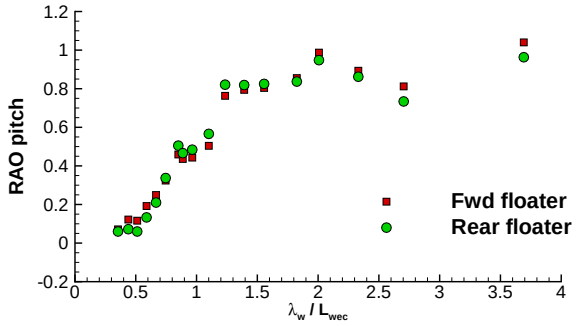

Fig. 13. Pitch RAO in regular waves.

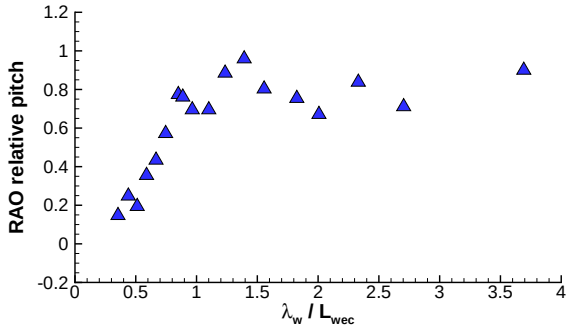

Fig. 14. RAO of the relative pitch rotation in regular waves.

with three floaters. Nonetheless, for the first floater, this peak for the heave RAO is shifted to an even smaller wavelength.

The calculation of the RAO for the relative pitch rotation is shown in Fig. 14 to be compared with those of the heave and pitch motions. More instructive is looking at the same data in dimensional form in Fig. 15. This dimensional RAO is rather interesting because it indicates at which frequency the conversion from wave energy to mechanical motion is more convenient. In the long wavelength regime, it reaches its maximum at wavelengths around 1.5 Hz.

From the experimental data, the relative displacements between the two floaters are calculated using geometrical relations which transform the motion at the CoG of the floaters into displacements at the edges of the linking beam. In this way, the tip displacement of the beam is computed with respect to the frame

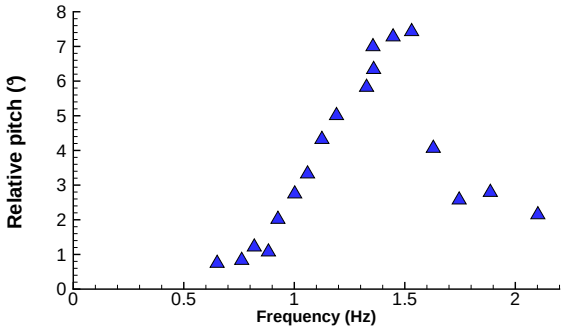

Fig. 15. Dimensional relative pitch rotation in regular waves.

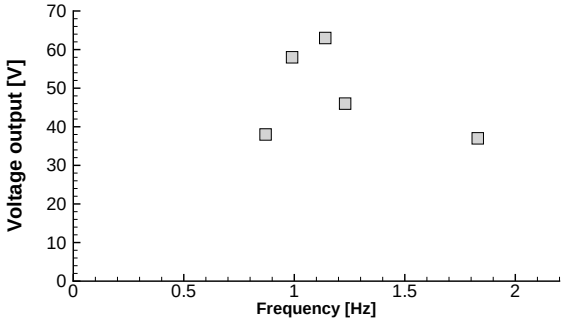

Fig. 16. Voltage output for selected regular waves for selected wave frequency in the neighbourhood of global maximum.

of reference having the origin O on the opposite end, and the local x-axis orthogonal to the barge vertical bulwark (it coincides with the beam axis at rest). The tip displacement time-history has been imposed to the free edge piezoelectric lamina modelled in COMSOL Multiphysics, while the edge at the bulwark was clamped. The voltage output has been calculated at the sea conditions reported in Table III. The results (Fig. 16) show that the voltage reaches the maximum value around 1.14 Hz, while the relative pitch peak occurs at a slightly higher frequency. The simulation also shows that the stress value imposed by the body motions is still compatible with the ultimate tensile strength of the junction, preventing from failures in the considered regular wave conditions.

TABLE III
REGULAR WAVE CASES CONSIDERED FOR PTO ANALYSIS.

Frequency [Hz]	**Wavelength** [m]	**Tip semi-amplitude** [m]
0.87	2.05	0.0124
0.99	1.55	0.0181
1.14	1.23	0.0196
1.23	0.97	0.0143
1.83	0.43	0.0116

VI. CONCLUSIONS

This paper is still a preliminary step toward the possibility of using piezoelectricity as PTO for extracting energy from waves. One interesting aspect is given by using small-scale testing which has required a new way of building the physical model, low-weight and low-cost sensors, and the design of a simple wave-maker. Even if the system at small scale is under current development, there are some important questions we need to face in the future: *i*) the way for upscaling the system so as to produce sufficient energy for user needs (local powering of sensors like a buoy); *ii*) the geometrical layout of the system, including the possibility to deploy an array of connected floaters; *iii*) the connection type to ensure that piezoelectric devices will not be subjected to high-stresses that may break the PZT lamina under off-design wave excitation.

REFERENCES

[1] A. F. de O. Falco, "Wave energy utilization: A review of the technologies," *Renewable Energy*, vol. 3, no. 14, pp. 899–918, 2010.
[2] L. Martinelli, B. Zanuttigh, and J. P. Kofoed, "Selection of design power of wave Energy converters based on wave basin experiments," *Renewable Energy*, vol. 11, no. 36, pp. 3124–3132, 2011.
[3] R. Henderson, "Design, simulation, and testing of a novel hydraulic power take-off system for the Pelamis wave Energy converter," *Renewable Energy*, vol. 2, no. 31, pp. 271–283, 2006.
[4] D. Elwood, S. C. Yim, J. Prudell, C. Stillinger, A. von Jouanne, T. Brekken, A. Brown, and R. Paasch, "Design, construction, and ocean testing of a taut-moored dual-body wave energy converter with a linear generator power take-off," *Renewable Energy*, vol. 2, no. 35, pp. 348–354, 2010.
[5] A. Jbaily and R. W. Yeung, "Piezoelectric devices for ocean energy: a brief survey," *Journal of Ocean Engineering and Marine Energy*, vol. 1, no. 1, pp. 101–118, 2015.
[6] C. B. Carroll, "Energy harvesting eel," July 23rd 2002, uS Patent 6,424,079.
[7] A. Koca and K. Erdoğan, "Performance analysis of wave energy harvesting system with piezoelectric element," in *International Conference Mechatronics*. Springer, 2017, pp. 743–749.
[8] D. A. Wang and H. Ko, "Piezoelectric energy harvesting from flow-induced vibration," *Journal of Micromechanics and Microengineering*, vol. 20, no. 2, p. 025019, 2010.
[9] A. S. Zurkinden, F. Campanile, and L. Martinelli, "Wave energy converter through piezoelectric polymers," in *Proceedings of the COMSOL Users Conference (Grenoble)*, 2007.
[10] X. D. Xie, Q. Wang, and N. Wu, "Potential of a piezoelectric energy harvester from sea waves," *Journal of Sound and Vibration*, vol. 333, no. 5, pp. 1421–1429, 2014.
[11] N. Okada, H. Fujimoto, S. Yabe, and M. Murai, "Experiments on floating wave-power generation using piezoelectric elements and pendulums in the water tank," in *OCEANS, 2012-Yeosu*. IEEE, 2012, pp. 1–8.
[12] C. Viñolo, D. Toma, A. Mànuel, and J. del Rio, "An ocean kinetic energy converter for low-power applications using piezoelectric disk elements," *The European Physical Journal Special Topics*, vol. 222, no. 7, pp. 1685–1698, 2013.
[13] C. Viñolo, D. Toma, A. Mànuel, and J. del Rio, "Sea motion electrical energy generator for low-power applications," in *OCEANS-Berger, 2013 MTS/IEEE*. IEEE, 2013, pp. 1–7.
[14] R. Murray and J. Rastegar, "Novel two-stage piezoelectric based ocean wave energy harvesters for moored or unmoored buoys," *Active and Passive Smart Structures and Integrated Systems*, vol. 7288, 2009.
[15] N. V. Viet and Q. Wang, "Ocean wave energy pitching harvester with a frequency tuning capability," *Energy*, vol. 162, pp. 603–617, 2018.
[16] N. V. Viet, N. Wu, and Q. Wang, "A review on energy harvesting from ocean waves by piezoelectric technology," *Journal of Modeling in Mechanics and Materials*, vol. 1, no. 2, 2017.
[17] H. Mutsuda, R. Watanabe, S. Azuma, Y. Tanaka, and Y. Doi, "Ocean power generator using flexible piezoelectric device," in *32nd International Conference on Ocean, Offshore and Artic Engineering*, Nantes, France, June 9–14 2013.
[18] D. Dessi, G. Leonardi, and F. Passacantilli, "Energy harvesting from waves using piezoelectric floaters," in *ASME 2018 37th International Conference on Ocean, Offshore and Arctic Engineering*. American Society of Mechanical Engineers, 2018, pp. V010T09A045–V010T09A045.

[19] D. Dessi, A. Carcaterra, and G. Diodati, "Experimental Investigation versus Numerical Simulation of the Dynamic Response of a Moored Floating Structure to Waves," in *218*, vol. 3. Institution of Mechanical Engineers Part M: Journal of Engineering for the Maritime Environment, 2004, pp. 153–165.